

EXPERIMENTS WITH LANCZOS BICONJUGATE A-ORTHONORMALIZATION METHODS FOR MOM DISCRETIZATIONS OF MAXWELL'S EQUATIONS

Y.-F. Jing

School of Mathematical Sciences
Institute of Computational Science
University of Electronic Science and Technology of China
Chengdu, Sichuan, 611731, China

B. Carpentieri

CRS4 Bioinformatics Laboratory
Edificio 3, Loc. Piscinamanna, Pula (CA) 09010, Italy

T.-Z. Huang

School of Mathematical Sciences
Institute of Computational Science
University of Electronic Science and Technology of China
Chengdu, Sichuan, 611731, China

Abstract—In this paper we consider a novel class of Krylov projection methods computed from the Lanczos biconjugate A-Orthonormalization procedure for the solution of dense complex non-Hermitian linear systems arising from the Method of Moments discretization of Maxwell's equations. We report on experiments on a set of model problems representative of realistic radar-cross section calculations to show their competitiveness with other popular Krylov solvers, especially when memory is a concern. The results presented in this study will contribute to assess the potential of iterative Krylov methods for solving electromagnetic scattering problems from large structures enriching the database of this technology.

1. INTRODUCTION

The quest of robust integral solvers for the Maxwell's equations is a critical component of the simulation in many realistic applications,

Corresponding author: B. Carpentieri (brunoc@crs4.it).

such as the Radar Cross Section (RCS) calculation of arbitrarily shaped objects like aircrafts, the design of radars and antennas, the study of sources of brain activity in biomagnetic and bioelectric inverse problems and many others. Boundary integral equations reformulate the standard Maxwell's equations in the frequency domain and compute the electric and the magnetic currents induced on the surface of the object whereas differential equation methods based on conventional finite differences, finite elements or finite volume techniques solve for the scattered fields. They require a simple description of the surface of the target by means of triangular facets (see an example of discretization in Figure 1), simplifying considerably the mesh generation especially in the case of moving objects. Rapid advances in computer technology and the introduction of novel algorithms with limited computational and memory requirement are giving a vigorous impulse to the development of boundary element techniques for solving electromagnetic (EM) scattering problems in two and three dimensions. From a linear algebra point of view, the bottleneck of the computation is the solution of large dense linear systems of equations generated by the Method of Moments (MoM) discretization of the integral equation for a given value of frequency [24]; MoM techniques are considered in many recent EM studies, see e.g., [9, 16, 27, 37, 53]. Out-of-core dense direct methods based on variants of Gaussian elimination can achieve reduced algorithmic complexity by solving for blocks of right-hand sides simultaneously [1, 7]. However, the memory cost of direct methods may limit the size of the tractable problem to a few hundred thousands unknowns on current computer systems. On the other hand, iterative Krylov methods only require matrix-vector (M-V) multiplications and can solve the problems of space. A straightforward

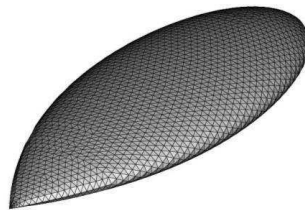


Figure 1. Example of surface discretization in an integral equation context. Each unknown of the problem is associated to an edge in the mesh. The geometry represents the ogive of a missile and has size 2.5 m. Courtesy of EADS-CCR Toulouse.

implementation of Krylov methods requires $\mathcal{O}(n^2)$ memory storage, where n is the number of unknowns, yielding a solution for one excitation. The Multilevel Fast Multipole Algorithm (MLFMA) [10, 11, 26, 50] can speedup the M-V product operation required at each iteration down to $\mathcal{O}(n \log n)$ algorithmic and memory complexity depending on the specific problem and implementation. Recent efforts to implement multipole techniques efficiently on distributed memory parallel computers have resulted in competitive application codes provably scalable to several million discretization points, e.g., the FISC code developed at University of Illinois [49–51], the INRIA/EADS integral equation code AS_ELFIP [54, 55], the Bilkent University code [14, 15], urging the quest of robust iterative algorithms for this problem class.

Many integral formulations for surface scattering and hybrid surface/volume discretizations yield non-Hermitian linear systems that cannot be solved using the Conjugate Gradient (CG) algorithm. The GMRES method [43] (or sometimes its flexible variant FGMRES [41]) is broadly used in application codes due to its robustness and smooth convergence, see e.g., the experiments reported in [6, 35] for solving very large boundary element equations involving million discretization points. On the other hand, iterative methods based on Lanczos biconjugation, such as BiCGSTAB [56] and QMR [20] can be cheaper in terms of memory requirements but may converge more slowly especially on realistic geometries [6, 36]. Choice of algorithm depends mostly on the specific application context and on the selected computer architecture. In this paper, we consider a novel class of Krylov projection methods based on the recently developed Lanczos A-orthonormalization procedure for solving dense complex non-Hermitian linear systems arising from the discretization of EM scattering problems expressed in an integral formulation. The first solver is named Biconjugate A-Orthogonal Residual (BiCOR). Two variants of BiCOR are also considered, which do not require multiplication by the Hermitian of A and may be well suited to use in combination with multipole techniques. They are the Conjugate A-Orthogonal Residual Squared (CORS) method and the Biconjugate A-Orthogonal Residual Stabilized (BiCORSTAB) method, see [29]. To the best of our knowledge, we are the first to report on this class of Krylov methods and to analyse their performance for solving the Maxwell's equations. The paper is structured as follows. In Section 2, we briefly introduce the Lanczos biconjugate A-orthonormalization procedure and the CORS, BiCOR, BiCORSTAB algorithms. In Section 3, we describe the integral equation context considered in this paper. In Section 4, we illustrate some numerical experiments

on a set of model problems arising in RCS calculation from complex structures and we analyse their performance against other popular algorithms derived from both Arnoldi orthogonalization and Lanczos biconjugation. Finally, in Section 5, we draw some conclusions arising from this study.

2. LANCZOS BICONJUGATE A-ORTHONORMALIZATION FOR LINEAR SYSTEMS

Krylov subspace methods search for approximate solutions of the linear system

$$Ax = b, \quad A \in \mathbb{C}^{n \times n} \text{ non-Hermitian}, \quad x, b \in \mathbb{C}^n, \quad (1)$$

in Krylov subspaces of increasing dimension. Denoting by $\mathcal{K}_i(A; v) \equiv \text{span}\{v, Av, \dots, A^{i-1}v\}$ the Krylov subspace of dimension i generated by A and v , the approximation x_m at step m belongs to $x_0 + K_m(A; v)$; v is typically chosen to be the (normalized) residual vector $r_0 = b - Ax_0$. We may write

$$x_m = x_0 + V_m y_m, \quad (2)$$

where the columns of V_m are the basis vectors of $K_m(A; v)$, and $y_m \in \mathbb{C}^m$ is the vector of coefficients of the linear combination. Krylov subspaces contain very good information about x because they are intimately related to the inverse of A , see e.g., [28]. Various methods differ in the way V_m and y_m are computed. In the *Ritz-Galerkin* approach, x_m is computed such that $b - Ax_m \perp K_m(A; r_0)$, leading to methods such as FOM and CG. The *minimum residual* approach minimizes $\|b - Ax_m\|_2$ over $K_m(A; r_0)$ leading to e.g., GMRES, MINRES. In the *Petrov-Galerkin* approach, the residual $r_m = b - Ax_m$ is orthogonal to other suitable m -dimensional subspaces, like e.g., in the popular Bi-CG and QMR algorithms. Finally, the *minimum error* approach minimizes the error $\|x - x_m\|_2$ over the subspace $A^H K_m(A^H; r_0)$, like in SYMMLQ and GMERR. See e.g., [12, 42].

In [29], a novel family of iterative Krylov methods for solving complex non-Hermitian linear systems is introduced. The approximate solution is searched in the Krylov subspace $K_m(A, r_0)$ by applying a Petrov-Galerkin approach and imposing the residual be orthogonal to the constraints subspace $A^H K_m(A^H, r_0^*)$. The shadow residual r_0^* is chosen to be equal to $P(A)r_0$, with $P(t)$ an arbitrary polynomial of certain degree with respect to the variable t (a default choice of $r_0^* = Ar_0$ will be adopted in this study if not otherwise clarified). The basis vector representations for the subspaces $K_m(A, r_0)$ and $A^H K_m(A^H, r_0^*)$ are computed by means of the Biconjugate A-Orthonormalization procedure. Starting from two vectors v_1 and w_1 chosen to satisfy

certain conditions, the method ideally builds up a pair of biconjugate A-orthonormal bases for the dual Krylov subspaces $K_m(A; v_1)$ and $K_m(A^H; w_1)$. It can be seen as an extension to complex non-Hermitian matrices of the A-biorthogonalization process introduced by Sogabe in [47]. We summarize the pseudocode in Algorithm 1. Throughout the paper, we denote by an overbar (“-”) the conjugate complex of a scalar, vector or matrix, and by the superscript “T” the transpose of a vector or matrix. Moreover, the standard Hermitian inner product of two complex vectors $u, v \in C^n$ is defined as

$$\langle u, v \rangle = u^H v = \sum_{i=1}^n \bar{u}_i v_i.$$

Algorithm 1 *Biconjugate A-Orthonormalization Procedure.*

- 1: Choose v_1, ω_1 , such that $\langle \omega_1, Av_1 \rangle = 1$
 - 2: Set $\beta_1 = \delta_1 \equiv 0, \omega_0 = v_0 = \mathbf{0} \in C^n$
 - 3: **for** $j = 1, 2, \dots$ **do**
 - 4: $\alpha_j = \langle \omega_j, A(Av_j) \rangle$
 - 5: $\hat{v}_{j+1} = Av_j - \alpha_j v_j - \beta_j v_{j-1}$
 - 6: $\hat{\omega}_{j+1} = A^H \omega_j - \bar{\alpha}_j \omega_j - \delta_j \omega_{j-1}$
 - 7: $\delta_{j+1} = |\langle \hat{\omega}_{j+1}, A\hat{v}_{j+1} \rangle|^{\frac{1}{2}}$
 - 8: $\beta_{j+1} = \frac{\langle \hat{\omega}_{j+1}, A\hat{v}_{j+1} \rangle}{\delta_{j+1}}$
 - 9: $v_{j+1} = \frac{\hat{v}_{j+1}}{\delta_{j+1}}$
 - 10: $\omega_{j+1} = \frac{\hat{\omega}_{j+1}}{\beta_{j+1}}$
 - 11: **end for**
-

The following proposition states some useful properties of Algorithm 1. For a detailed proof, see [29].

Proposition 1 *If Algorithm 1 proceeds m steps, then the right and left Lanczos-type vectors $v_j, j = 1, 2, \dots, m$ and $w_i, i = 1, 2, \dots, m$ form a biconjugate A-orthonormal system in exact arithmetic, i.e.,*

$$\langle \omega_i, Av_j \rangle = \delta_{i,j}, \quad 1 \leq i, j \leq m.$$

Furthermore, denote by $V_m = [v_1, v_2, \dots, v_m]$ and $W_m = [w_1, w_2, \dots, w_m]$ the $n \times m$ matrices and by \underline{T}_m the extended tridiagonal matrix of the form

$$\underline{T}_m = \begin{bmatrix} T_m & \\ & \delta_{m+1} e_m^T \end{bmatrix},$$

where

$$T_m = \begin{bmatrix} \alpha_1 & \beta_2 & & & & \\ \delta_2 & \alpha_2 & \beta_3 & & & \\ & \ddots & \ddots & \ddots & & \\ & & \delta_{m-1} & \alpha_{m-1} & \beta_m & \\ & & & \delta_m & \alpha_m & \end{bmatrix},$$

whose entries are the coefficients generated during the algorithm implementation, and in which $\alpha_1, \dots, \alpha_m, \beta_2, \dots, \beta_m$ are complex while $\delta_2, \dots, \delta_m$ positive. Then with the Biconjugate *A*-Orthonormalization Procedure, the following four relations hold

$$AV_m = V_m T_m + \delta_{m+1} v_{m+1} e_m^T \tag{3}$$

$$A^H W_m = W_m T_m^H + \bar{\beta}_{m+1} \omega_{m+1} e_m^T \tag{4}$$

$$W_m^H AV_m = I_m \tag{5}$$

$$W_m^H A^2 V_m = T_m \tag{6}$$

From Proposition 1, a family of Krylov methods for linear systems based on Algorithm 1 can be designed along the following lines. Recall that we consider an oblique projection method onto $K_m(A, v_1)$ and orthogonally to $L_m = A^H K_m(A^H, \omega_1)$ where $v_1 = \frac{r_0}{\|r_0\|_2}$ and ω_1 is chosen arbitrarily such that $\langle \omega_1, Av_1 \rangle \neq 0$. But ω_1 is often chosen to be equal to $\frac{Av_1}{\|Av_1\|_2^2}$ subjecting to $\langle \omega_1, Av_1 \rangle = 1$. Run Algorithm 1 m steps and seek an m th approximate solution from the affine subspace $x_0 + K_m(A, v_1)$ of dimension m , by imposing the Petrov-Galerkin condition

$$b - Ax_m \perp L_m,$$

which can be mathematically written in matrix formulation as

$$(A^H W_m)^H (b - Ax_m) = 0, \tag{7}$$

where W_m is defined in Proposition 1. Since the approximate solution can be represented as in (2), where V_m is defined in Proposition 1 and $y_m \in \mathbb{C}^m$ contains the coefficients of the linear combination, by simple substitution and computation with Eqs. (6)–(7), a tridiagonal system for solving y_m is resulted as

$$T_m y_m = \beta e_1,$$

where T_m is formed in Proposition 1, and $\beta = \|r_0\|_2$. The whole iterative scheme is sketched in Algorithm 2.

The BiCOR method is derived by imposing the biorthogonality and biconjugacy conditions, and taking the strategy of reducing the number of M-V multiplications by introducing an auxiliary vector

Algorithm 2 *Two-sided Biconjugate A-Orthonormalization method.*

-
- 1: Compute $r_0 = b - Ax_0$ for some initial guess x_0 and set $\beta = \|r_0\|_2$.
 - 2: Start with $v_1 = \frac{r_0}{\beta}$ and choose ω_1 such that $\langle \omega_1, Av_1 \rangle = 1$, (for example, $\omega_1 = \frac{Av_1}{\|Av_1\|_2^2}$)
 - 3: Generate the Lanczos-type vectors v_1, v_2, \dots, v_m and $\omega_1, \omega_2, \dots, \omega_m$ as well as the tridiagonal matrix T_m by running Algorithm 1 m steps.
 - 4: Compute $y_m = T_m^{-1}(\beta e_1)$ and $x_m = x_0 + V_m y_m$
-

recurrence [29]. We sketch a pseudocode of BiCOR in Algorithm 3. One iteration requires one M-V product by A and one by A^H . Indeed the M-V products by A^H may be tricky to implement with some implementations of MLFMA. Therefore two variants of the BiCOR method which require M-V products only by A , namely the CORS and the BiCORSTAB methods, are considered in this study. They may also make BiCOR more effective in certain circumstances. The CORS method is mathematically equivalent to CRS [48] but can lead to considerably smoother convergence behavior, as well as to the CGS [52] and SCGS methods [47], and may be amazingly competitive with the BiCGSTAB method. However, like the CGS, SCGS, and CRS methods, it is based on squaring the residual polynomial. In cases of irregular convergence, this may lead to substantial build-up of rounding errors and worse approximate solutions, or possibly even overflow. The pseudocode for the preconditioned CORS method with a left preconditioner M can be represented by the Algorithm 4. A more smoothly converging variant of the BiCOR method, the BiCORSTAB method, is developed as an attempt to remedy this difficulty and to cure to some extent some of the numerical problems that plague the CORS method without giving up the attractive speed of convergence of CORS. The BiCORSTAB method is a polynomial product variant of the BiCOR method, which is adapted easily from the BiCGSTAB method [17, 42, 56]. The pseudocode for the left preconditioned BiCORSTAB algorithm is shown in Algorithm 5. Compared to the BiCGSTAB method, the convergence behaviour of the BiCORSTAB method in certain cases is much smoother so that it sometimes produces much more accurate residual vectors (and, hence, better approximate solutions). And it may even converge considerably faster than the BiCGSTAB method. However, in each iteration the BiCORSTAB method requires two more additional operations for vector updates [29].

Algorithm 3 *Left preconditioned BiCOR method.*

```

1: Compute  $r_0 = b - Ax_0$  for some initial guess  $x_0$ .
2: Choose  $r_0^* = P(A)r_0$  such that  $\langle r_0^*, Ar_0 \rangle \neq 0$ , where  $P(t)$  is a
   polynomial in  $t$ . (For example,  $r_0^* = Ar_0$ ).
3: for  $j = 1, 2, \dots$  do
4:   solve  $Mz_{j-1} = r_{j-1}$ 
5:   if  $j=1$  then
6:     solve  $M^H z_0^* = r_0^*$ 
7:   end if
8:    $\hat{z} = Az_{j-1}$ 
9:    $\rho_{j-1} = \langle z_{j-1}^*, \hat{z} \rangle$ 
10:  if  $\rho_{j-1} = 0$ , method fails
11:  if  $j = 1$  then
12:     $p_0 = z_0$ 
13:     $p_0^* = z_0^*$ 
14:     $q_0 = \hat{z}$ 
15:  else
16:     $\beta_{j-2} = \rho_{j-1} / \rho_{j-2}$ 
17:     $p_{j-1} = z_{j-1} + \beta_{j-2} p_{j-2}$ 
18:     $p_{j-1}^* = z_{j-1}^* + \beta_{j-2} p_{j-2}^*$ 
19:     $q_{j-1} = \hat{z} + \beta_{j-2} q_{j-2}$ 
20:  end if
21:   $q_{j-1}^* = A^H p_{j-1}^*$ 
22:  solve  $M^H u_{j-1}^* = q_{j-1}^*$ 
23:   $\alpha_{j-1} = \rho_{j-1} / \langle u_{j-1}^*, q_{j-1} \rangle$ 
24:   $x_j = x_{j-1} + \alpha_{j-1} p_{j-1}$ 
25:   $r_j = r_{j-1} - \alpha_{j-1} q_{j-1}$ 
26:   $z_j^* = z_{j-1}^* - \bar{\alpha}_{j-1} u_{j-1}^*$ 
27:  check convergence; continue if necessary
28: end for

```

3. THE INTEGRAL EQUATION CONTEXT

We consider the following reformulation of the standard Maxwell's problem for EM scattering in the frequency domain:

Find the surface current \vec{j} such that for all tangential test functions

Algorithm 4 *Left preconditioned CORS method.*

```

1: Compute  $r_0 = b - Ax_0$  for some initial guess  $x_0$ .
2: Choose  $r_0^* = P(A)r_0$  such that  $\langle r_0^*, Ar_0 \rangle \neq 0$ , where  $P(t)$  is a
   polynomial in  $t$ . (For example,  $r_0^* = Ar_0$ ).
3: for  $j = 1, 2, \dots$  do
4:   solve  $Mz_{j-1} = r_{j-1}$ 
5:    $\hat{r} = Az_{j-1}$ 
6:    $\rho_{j-1} = \langle r_0^*, \hat{r} \rangle$ 
7:   if  $\rho_{j-1} = 0$ , method fails
8:   if  $j = 1$  then
9:      $e_0 = r_0$ 
10:    solve  $Mze_0 = e_0$ 
11:     $d_0 = \hat{r}$ 
12:     $q_0 = \hat{r}$ 
13:  else
14:     $\beta_{j-2} = \rho_{j-1} / \rho_{j-2}$ 
15:     $e_{j-1} = r_{j-1} + \beta_{j-2}h_{j-2}$ 
16:     $ze_{j-1} = z_{j-1} + \beta_{j-2}zh_{j-2}$ 
17:     $d_{j-1} = \hat{r} + \beta_{j-2}f_{j-2}$ 
18:     $q_{j-1} = d_{j-1} + \beta_{j-2}(f_{j-2} + \beta_{j-2}q_{j-2})$ 
19:  end if
20:  solve  $Mq = q_{j-1}$ 
21:   $\hat{q} = Aq$ 
22:   $\alpha_{j-1} = \rho_{j-1} / \langle r_0^*, \hat{q} \rangle$ 
23:   $h_{j-1} = e_{j-1} - \alpha_{j-1}q_{j-1}$ 
24:   $zh_{j-1} = ze_{j-1} - \alpha_{j-1}q$ 
25:   $f_{j-1} = d_{j-1} - \alpha_{j-1}\hat{q}$ 
26:   $x_j = x_{j-1} + \alpha_{j-1}(2ze_{j-1} - \alpha_{j-1}q)$ 
27:   $r_j = r_{j-1} - \alpha_{j-1}(2d_{j-1} - \alpha_{j-1}\hat{q})$ 
28:  check convergence; continue if necessary
29: end for

```

\vec{j}^t , we have

$$\begin{aligned}
& \int_{\Gamma} \int_{\Gamma} G(|y-x|) \left(\vec{j}(x) \cdot \vec{j}^t(y) - \frac{1}{k^2} \operatorname{div}_{\Gamma} \vec{j}(x) \cdot \operatorname{div}_{\Gamma} \vec{j}^t(y) \right) dx dy \\
&= \frac{i}{kZ_0} \int_{\Gamma} \vec{E}_{inc}(x) \cdot \vec{j}^t(x) dx.
\end{aligned} \tag{8}$$

We denote by $G(|y-x|) = \frac{e^{ik|y-x|}}{4\pi|y-x|}$ the Green's function of Helmholtz equation, Γ the boundary of the object, k the wave number and $Z_0 = \sqrt{\mu_0/\epsilon_0}$ the characteristic impedance of vacuum (ϵ is the electric permittivity and μ the magnetic

Algorithm 5 *Left preconditioned BiCORSTAB method.*

```

1: Compute  $r_0 = b - Ax_0$  for some initial guess  $x_0$ .
2: Choose  $r_0^* = P(A)r_0$  such that  $\langle r_0^*, Ar_0 \rangle \neq 0$ , where  $P(t)$  is a
   polynomial in  $t$ . (For example,  $r_0^* = Ar_0$ ).
3: for  $j = 1, 2, \dots$  do
4:    $\hat{r} = Ar_{j-1}$ 
5:    $\rho_{j-1} = \langle r_0^*, \hat{r} \rangle$ 
6:   if  $\rho_{j-1} = 0$ , method fails
7:   if  $j = 1$  then
8:      $p_0 = r_0$ 
9:      $q_0 = \hat{r}$ 
10:  else
11:     $\beta_{j-2} = (\rho_{j-1}/\rho_{j-2}) \times (\alpha_{j-2}/\omega_{j-2})$ 
12:     $p_{j-1} = r_{j-1} + \beta_{j-2} (p_{j-2} - \omega_{j-2}q_{j-2})$ 
13:     $q_{j-1} = \hat{r} + \beta_{j-2} (q_{j-2} - \omega_{j-2}\hat{q}_{j-2})$ 
14:  end if
15:  solve  $M\hat{p} = p_{j-1}$ 
16:   $\hat{q}_{j-1} = Aq_{j-1}$ 
17:   $\alpha_{j-1} = \rho_{j-1} / \langle r_0^*, \hat{q}_{j-1} \rangle$ 
18:   $s = r_{j-1} - \alpha_{j-1}q_{j-1}$ 
19:  check norm of  $s$ ; if small enough: set  $x_j = x_{j-1} + \alpha_{j-1}\hat{p}$  and stop
20:  solve  $M\hat{s} = s$ 
21:   $t = \hat{r} - \alpha_{j-1}\hat{q}_{j-1}$ 
22:   $\omega_{j-1} = \langle t, s \rangle / \langle t, t \rangle$ 
23:   $x_j = x_{j-1} + \alpha_{j-1}\hat{p} + \omega_{j-1}\hat{s}$ 
24:   $r_j = s - \omega_{j-1}t$ 
25:  check convergence; continue if necessary
   for continuation it is necessary that  $\omega_{j-1} \neq 0$ 
26: end for

```

permeability). Given a continuously differentiable vector field $\vec{j}(x)$ represented in Cartesian coordinates on a 3D Euclidean space as $\vec{j}(x_1, x_2, x_3) = j_{x_1}(x_1, x_2, x_3)\vec{e}_{x_1} + j_{x_2}(x_1, x_2, x_3)\vec{e}_{x_2} + j_{x_3}(x_1, x_2, x_3)\vec{e}_{x_3}$, where \vec{e}_{x_1} , \vec{e}_{x_2} , \vec{e}_{x_3} are the unit basis vectors of the Euclidean space, we denote by $\text{div}\vec{j}(x)$ the divergence operator defined as

$$\text{div}\vec{j}(x) = \frac{\partial j_{x_1}}{\partial x_1} + \frac{\partial j_{x_2}}{\partial x_2} + \frac{\partial j_{x_3}}{\partial x_3}.$$

Eq. (8) expresses the electric currents in terms of the electric field and is called Electric Field Integral Equation (EFIE). It is applied to arbitrary geometries like objects with cavities, disconnected parts, breaks on the surface [3, 33].

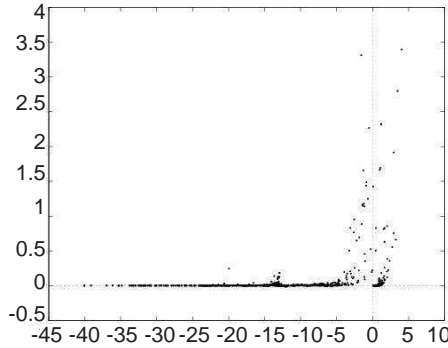


Figure 2. Example of spectrum for the EFIE operator on a model problem representative of the general trend.

On discretizing Eq. (8) in space by the MoM over a mesh containing n edges, the surface current \vec{j} is expanded into a set of basis functions $\{\vec{\varphi}_i\}_{1 \leq i \leq n}$ with compact support (the Rao-Wilton-Glisson basis [40] is a popular choice), then the integral equation is applied to a set of tangential test functions \vec{j}^t . Selecting $\vec{j}^t = \vec{\varphi}_j$, we are led to compute the set of coefficients $\{\lambda_i\}_{1 \leq i \leq n}$ such that

$$\sum_{1 \leq i \leq n} \lambda_i \left[\int_{\Gamma} \int_{\Gamma} G(|y-x|) \left(\vec{\varphi}_i(x) \cdot \vec{\varphi}_j(x) - \frac{1}{k^2} \text{div}_{\Gamma} \vec{\varphi}_i(x) \cdot \text{div}_{\Gamma} \vec{\varphi}_j(y) \right) dx dy \right] = \frac{i}{kZ_0} \int_{\Gamma} \vec{E}_{inc}(x) \cdot \vec{\varphi}_j(x) dx, \tag{9}$$

for each $1 \leq i \leq n$. The set of Eq. (9) can be recast in matrix form as

$$A\lambda = b, \tag{10}$$

where $A = [A_{ij}]$ and $b = [b_i]$ have elements

$$A_{ij} = \int_{\Gamma} \int_{\Gamma} G(|y-x|) \left(\vec{\varphi}_i(x) \cdot \vec{\varphi}_j(y) - \frac{1}{k^2} \text{div}_{\Gamma} \vec{\varphi}_i(x) \cdot \text{div}_{\Gamma} \vec{\varphi}_j(y) \right) dx dy, \\ b_j = \frac{i}{kZ_0} \int_{\Gamma} \vec{E}_{inc}(x) \cdot \vec{\varphi}_j(y) dx.$$

In Eq. (10), the set of unknowns are associated with the vectorial flux across an edge in the mesh. The coefficient matrix A generated by MoM is dense complex symmetric (but non-Hermitian). The right-hand side varies with the frequency and the direction of the illuminating wave.

Linear systems issued from boundary element discretizations of Maxwell's equations are typically very large in applications although they can be much smaller compared to those arising from FE or FV formulations of the same problem. The number of unknowns n grows linearly with the size of the scatterer and quadratically with the frequency of the incoming radiation [2]. Scattering simulations involving targets of size in the order of a few tens of wavelength illuminated at approximately one GHz of frequency may lead to meshes with many million points [54] and yield dense matrices containing several Tbytes of data. The condition number of the pertinent linear system can grow like $p^{1/2}$, where p denotes the size of the scatterer in terms of the wavelength, and linearly with the number of points per wavelength [8]. In Figure 2 we show the distribution of eigenvalues of the discretization matrix arising for EFIE operators. The presence of many isolated eigenvalues, some close to the origin and many with large negative real part is notoriously unfavorable to have rapid convergence of Krylov methods, see e.g., [25]. In fact, when the number of unknowns n is related to the wavenumber the iteration count of iterative solvers may increase as $\mathcal{O}(n^{0.5})$ [49].

Besides EFIE other formulations are possible for modeling closed targets, like e.g., the Magnetic Field Integral Equation (MFIE) which reads

$$\int_{\Gamma} \left(\vec{R}_{ext} j \wedge \vec{\nu} \right) \cdot \vec{j}^t + \frac{1}{2} \int_{\Gamma} \vec{j} \cdot \vec{j}^t = - \int_{\Gamma} \left(\vec{H}_{inc} \wedge \vec{\nu} \right) \cdot \vec{j}^t.$$

The operator $\vec{R}_{ext} j$ is defined as

$$\vec{R}_{ext} j(y) = \int_{\Gamma} \text{grad}_y G(|y-x|) \wedge \vec{j}(x) dx,$$

and is evaluated in the domain exterior to the object. Both EFIE and MFIE suffer from interior resonances which make the numerical solution problematic at some frequencies known as resonant frequencies, especially for large objects. The problem can be solved by combining linearly EFIE and MFIE. The resulting integral equation is known as Combined Field Integral Equation (CFIE) and is the formulation of choice for closed targets. Hybrid approaches are also possible, see e.g., [18]. On CFIE the number of iterations typically increases more slowly, as $\mathcal{O}(n^{0.25})$, and the performance of other Krylov subspace methods are reported to be more or less equivalent in terms of the number of matrix-vector products, see e.g., comments in [36]. Therefore, we focus our study on EFIE.

4. NUMERICAL EXPERIMENTS

The set of linear systems selected for the numerical experiments arise from RCS calculations of realistic targets. They are dense complex non-Hermitian. The geometries are depicted in Figure 3 and we report the characteristics of the model problems in Table 1. Although not very large, the selected problems are representative of realistic RCS calculation. Their solution demands considerable computer resources. For the Airbus A318 problem, storing the pertinent linear system requires around 18 Gb of RAM when symmetry is not exploited. Larger

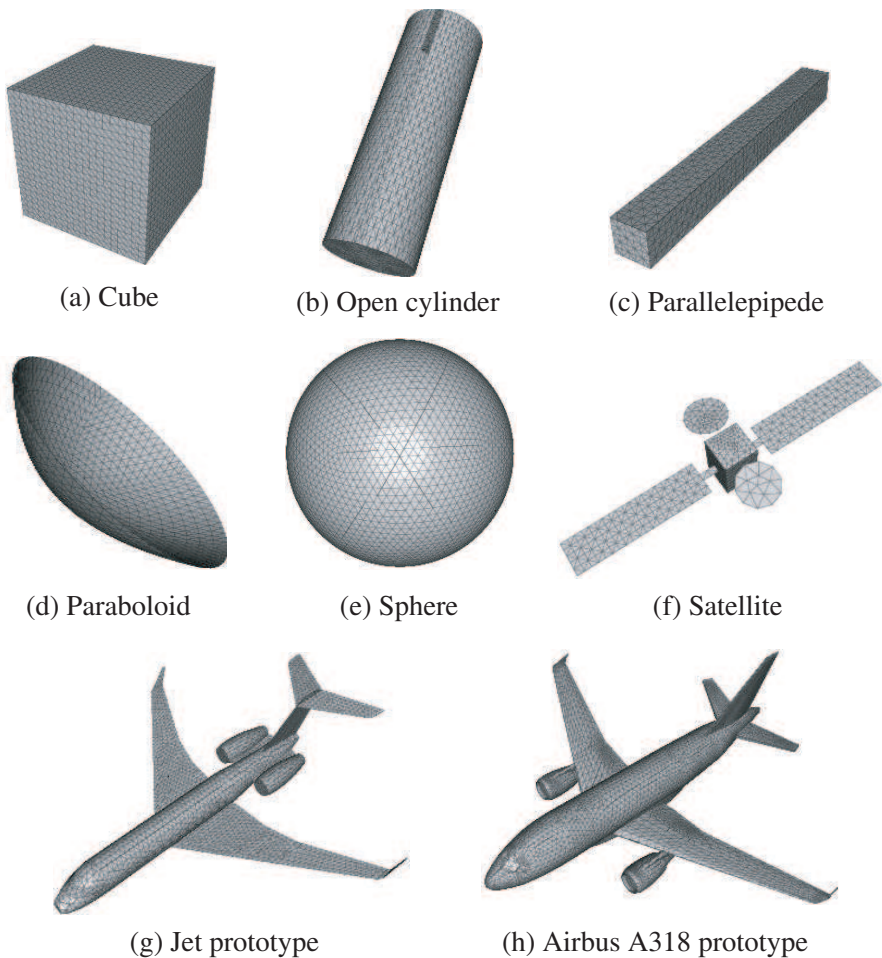


Figure 3. Meshes associated with test examples.

Table 1. Characteristics of the model problems.

Example	Description	Size	Frequency (MHz)	$\kappa_1(A)$	Geometry
1	Cube	7200	249	$2 \cdot \mathcal{O}(10^5)$	Fig. 3(a)
2	Open cylinder	6268	362	$1 \cdot \mathcal{O}(10^5)$	Fig. 3(b)
3	Parallelepiped	3150	621	$6 \cdot \mathcal{O}(10^5)$	Fig. 3(c)
4	Paraboloid	1980	711	$9 \cdot \mathcal{O}(10^3)$	Fig. 3(d)
5	Sphere	12000	535	$6 \cdot \mathcal{O}(10^5)$	Fig. 3(e)
6	Satellite	1699	57	$1 \cdot \mathcal{O}(10^5)$	Fig. 3(f)
7	Jet prototype	7924	615	$1 \cdot \mathcal{O}(10^7)$	Fig. 3(g)
8	Airbus A318 prototype	23676	800	$1 \cdot \mathcal{O}(10^7)$	Fig. 3(h)

Table 2. Algorithmic cost and memory expenses of the implementation of Krylov algorithms that are used for the experiments. We denote by n the problem size and by i the iteration number.

Solver	Type	Products by A	Products by A^H	Memory	Reference
BiCOR	general	1	1	matrix+ $10n$	[29]
CORS	"	2	-	matrix+ $14n$	[29]
BiCORSTAB	"	2	-	matrix+ $13n$	[29]
GMRES	"	1	-	matrix + $(i+5)n$	[43]
QMR	"	2	1	matrix+ $11n$	[21]
TFQMR	"	4	-	matrix+ $10n$	[19]
BiCGSTAB	"	2	-	matrix+ $7n$	[56]
BiCGSTAB (l)	"	$2l$	-	matrix + $2l+5$	[46]
SQMR	symmetric	1	-	matrix+ $10n$	[22]

problems require to use MLFMA for the M-V products to reduce the memory requirement and effective preconditioners to accelerate the convergence, and they are out of the scope of this study. We carry out the M-V product at each iteration using dense linear algebra packages, i.e., the ZGEMV routine available in the LAPACK library and we do not use preconditioning. In addition to BiCOR, CORS and BiCORSTAB, we consider complex versions of iterative algorithms

based on Lanczos biorthogonalization, such as BiCGSTAB and QMR, and on Arnoldi orthogonalization, such as GMRES. In Table 2, we list the complete set of solvers used in our experiments. All the runs are done on one node of the *Entu* cluster facility located at CRS4. Each node features a quad core Intel CPU at 2.8 GHz and 16 GB of physical RAM. The codes are compiled in Fortran with the Portland Group Fortran 90 compiler version 9.

4.1. Discussions

In Table 3, we show the number of iterations required by Krylov methods to reduce the initial residual to $\mathcal{O}(10^{-5})$ starting from the zero vector. The right-hand side of the linear system is set up so that the initial solution is the vector of all ones. We observe the effectiveness

Table 3. Number of iterations and CPU time (in seconds) required by Krylov methods to reduce the initial residual to $\mathcal{O}(10^{-5})$. For each example, an asterisk “*” indicates the fastest run.

Solver/ Example	1	2	3	4	5	6
CORS	380 (211*)	601 (253*)	148 (16*)	197 (9)	294 (451*)	371 (11*)
BiCOR	441 (251)	785 (334)	226 (25)	232 (10)	338 (525)	431 (15)
BiCORSTAB	640 (525)	941 (614)	239 (40)	261 (20)	423 (1099)	775 (37)
GMRES(50)	>3000 (> 844)	2191 (469)	289 (16*)	261 (6*)	1803 (1397)	871 (17)
QMR	615 (508)	878 (548)	239 (38)	255 (16)	430 (1045)	452 (24)
TFQMR	399 (435)	482 (398)	146 (32)	177 (15)	281 (863)	373 (27)
BiCGSTAB	764 (418)	1065 (444)	265 (28)	234 (10)	680 (1031)	566 (18)

Table 4. Number of iterations and CPU time (in seconds) required by restarted GMRES for different values of restart to reduce the initial residual to $\mathcal{O}(10^{-5})$. For each example, an asterisk “*” indicates the fastest run.

Example/ Solver	GMRES (50)	GMRES (100)	GMRES (200)	GMRES (500)
1	> 3000 (> 844)	2182 (790)	374 (106)	296 (86*)
2	2191 (469)	1060 (268)	702 (153)	411 (94*)
3	289 (16)	228 (13)	176 (10*)	176 (10*)
4	261 (6)	217 (5)	182 (4*)	182 (4*)
5	1803 (1397)	654 (504)	378 (293)	292 (228*)
6	871 (17)	608 (12)	470 (9)	306 (6*)

of the CORS method, that is the fastest non-Hermitian solver with respect to CPU time on most selected examples except GMRES with large restart. Indeed, unrestarted GMRES may outperform all other Krylov methods and should be used when memory is not a concern. However reorthogonalization costs may penalize the GMRES convergence in large-scale applications, so using high values of restart may not be convenient (or even not affordable for the memory) as shown in earlier studies [6]. In Table 3, we select a value of 50 for the restart parameter; for the sake of completeness in Table 4 we show results using higher restart. The good efficiency of CORS is even more evident on the two realistic aircraft problems i.e., Examples 3(g)–3(h) which are very difficult to solve by iterative methods as no convergence is obtained without preconditioning in 3000 iterates. In Table 6 we report on the number of iterations and on the CPU time to reduce the initial residual to $\mathcal{O}(10^{-3})$. This tolerance may be considered accurate enough for engineering purposes. In [6] it has been shown that a level of accuracy of $\mathcal{O}(10^{-3})$ may enable a correct reconstruction of the radar cross section of the object. Again, CORS is more efficient than

Table 5. Number of iterations and CPU time (in seconds) required by BiCGSTAB (l) for different levels l to reduce the initial residual to $\mathcal{O}(10^{-5})$. For each example, an asterisk “*” indicates the fastest run.

Example/Solver	BiCGSTAB (1)	BiCGSTAB (2)	BiCGSTAB (3)	BiCGSTAB (4)
1	764 (418)	367 (402)	234 (383*)	181 (394)
2	1065 (444)	512 (424)	324 (404*)	245 (405)
3	265 (28)	123 (26)	81 (26)	60 (25*)
4	234 (10)	121 (10)	77 (10)	56 (9*)
5	680 (1031)	319 (966)	199 (898)	139 (835*)
6	566 (18)	268 (17)	170 (16*)	127 (16*)

Table 6. Number of iterations and CPU time (in seconds) for CORS and GMRES (50) to reduce the initial residual to $\mathcal{O}(10^{-3})$ on the two aircraft problems 3(g) and 3(h). These problems do not converge in 3000 iterations. For each example, an asterisk “*” indicates the fastest run.

Example/Solver	CORS	GMRES50
7	1286 (981*)	>3000 (>1147)
8	924 (5493*)	2792 (8645)

restarted GMRES on these two tough problems.

The BiCOR method also shows fast convergence and may be an appropriate choice. Both CORS and BiCOR are based on short-term recurrences and therefore they are very cheap in memory. A nice feature of CORS over BiCOR is that it does not require matrix multiplications by A^H . This may represent an advantage when MLFMA is used because the Hermitian product often requires a specific algorithmic implementation [54]. In Figure 4 we illustrate the convergence history of CORS and GMRES (50) on Examples 3 and 6 to show the different numerical behavior of the two families of solvers. The residual reduction is much smoother for GMRES along the iterations. We also observe from Table 7 that different choices of the initial shadow residual may further reduce the overall solution time. However, the optimal choice is problem dependent and may be found on a trial and error basis.

Methods based on Lanczos biconjugation are also considered in many scattering analysis, mainly for their simplicity (parameter-free) and low memory requirements. The Illinois Group reports on successful results with BiCG in conjunction with preconditioners and MLFMA to

Table 7. Number of iterations and CPU time (in seconds) for the CORS method using different choice of initial shadow residual.

Example/Choice for $P(t)$	$r_0^* = r_0$	$r_0^* = A \cdot r_0$
1	419 (234)	380 (211)
2	473 (209)	601 (253)
7	1103 (726)	1286 (981)

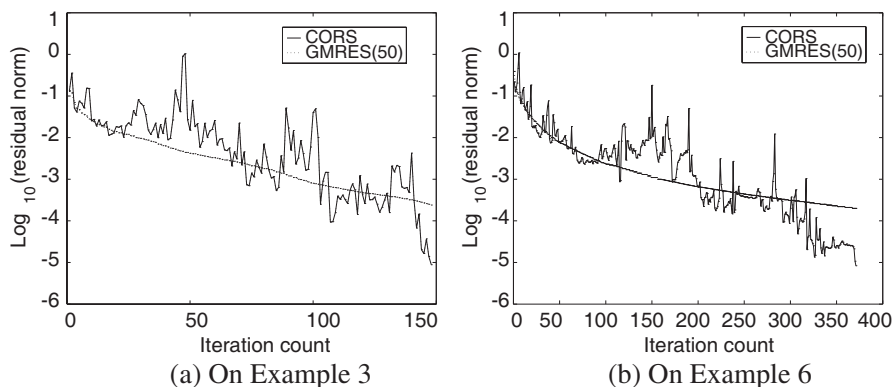


Figure 4. Convergence histories for CORS and GMRES.

solve the EFIE [23, 34, 44, 50]. The BiCGSTAB method preconditioned with approximate inverse is robust and converges very fast for solving electromagnetic wave scattering by 3D dielectric and conducting objects via hybrid surface and volume integral equations [31, 32], as well as for solving boundary element formulations of bioelectric and biomagnetic inverse problems in Magnetoencephalography (MEG) in combination with incomplete factorization techniques [39]. In our experiments, as shown in Table 5, BiCGSTAB and its enhanced variant BiCGSTAB (*l*) [46] is less efficient than BiCOR and CORS. Also, it often requires more iterations to converge than BiCORSTAB although each iteration is slightly less expensive as mentioned in Section 2.

QMR-like methods are also popular for this problem class [38, 54]. From the results shown in Table 3, though, we observe that nonsymmetric QMR algorithms generally converge more slowly than GMRES, BiCOR, CORS. For the sake of completeness, in Table 8 we report on results with a symmetric variant of QMR (referred to as SQMR) that exploits the system symmetry achieving high efficiency in our runs. One problem with SQMR is that it needs a symmetric preconditioner which may be restrictive. Indeed many effective algebraic preconditioners for surface integral equations are nonsymmetric and therefore they cannot be used with SQMR. And even in the case a symmetric preconditioner is available, due to round-off errors the multipole operator of MLFMA often loses the theoretical symmetry of EFIE leading to divergence of SQMR as shown in the experiments reported in [13]. However, when symmetry is preserved and a symmetric preconditioner is used, SQMR is the most efficient solver being very competitive with full GMRES.

Preconditioning is critical for EFIE to drastically reduce the large number of iterations of Krylov methods. This issue has been investigated in many studies. Simple preconditioners like the diagonal of A , diagonal blocks, or a band can be effective only when the coefficient matrix arising from the discretization of the integral formulation has some degree of diagonal dominance [50]. Incomplete factorizations have been successfully applied to solve nonsymmetric dense systems in [45] and hybrid integral formulations in [31], and also for solving the EFIE provided pivoting is used [36]. Approximate inverse methods are

Table 8. Number of iterations and CPU time (in seconds) required by SQMR to reduce the initial residual to $\mathcal{O}(10^{-5})$.

Solver/Example	1	2	3	4	5	6
SQMR	224 (61)	416 (87)	129 (7)	103 (2)	201 (152)	405 (6)

Table 9. Experiments with a physical right-hand side.

Example 2			
φ	CORS	GMRES (50)	BiCGSTAB
0	465	2843	1303
$\frac{\pi}{2}$	465	2969	1303
Example 3			
φ	CORS	GMRES (50)	BiCGSTAB
0	169	348	263
$\frac{\pi}{2}$	176	348	259
Example 6			
φ	CORS	GMRES (50)	BiCGSTAB
0	426	1600	562
$\frac{\pi}{2}$	452	1500	534

generally less prone to instabilities on indefinite systems, and several preconditioners of this type have been proposed in electromagnetism (see for instance [4, 6, 30]). Choice of algorithm depends on the specific problem and on the selected computer architecture. However, experiments show that preconditioning does not change the relative merits of Krylov algorithms, see e.g., [5, 6, 36]. For this reason we do not use any specific preconditioner in this study to keep the comparison as general as possible.

Finally, in Table 9 we report on experiments using physical right-hand sides computed from Eq. (10). We take as incident field a plane wave of general form in spherical coordinates

$$\vec{E}_{inc}(x, \varphi, p_\theta, p_\varphi) = (p_\theta)\hat{u}_\theta e^{ikx \cdot \hat{u}_r(\varphi)} + (p_\varphi)e^{ikx \cdot \hat{u}_r(\varphi)},$$

where (p_θ, p_φ) are two complex numbers and $\hat{u}_r; \hat{u}_\theta; \hat{u}_\varphi$ are the unitary vectors:

$$\hat{u}_r = \begin{pmatrix} \cos \varphi \cos \theta \\ \sin \varphi \cos \theta \\ \sin \theta \end{pmatrix}, \hat{u}_\theta = \begin{pmatrix} -\cos \varphi \sin \theta \\ -\sin \varphi \sin \theta \\ \cos \theta \end{pmatrix}, \hat{u}_\varphi = \begin{pmatrix} -\sin \varphi \cos \theta \\ -\cos \varphi \cos \theta \\ \sin \theta \end{pmatrix},$$

Without loss of generality, we may take $\theta = 0$ and φ variable from 0 to 2π leading to the following expression for the incident field

$$\vec{E}_{inc}(x) = \vec{E}_{inc}(x, \varphi) = \hat{z}e^{ikx \cdot \hat{u}_r(\varphi)} = \hat{z}e^{ik(x_1 \cos \varphi + x_2 \sin \varphi)}.$$

We see in Table 9 that the number of iterations may change significantly, especially for open surfaces. However, the trend is confirmed and the CORS method remains very competitive with the other Krylov algorithms.

5. CONCLUSION

In this study we have discussed iterative solution strategies for EM scattering problems expressed in an integral formulation. We have analyzed the performance of a class of orthogonal projection Krylov algorithms computed from the Lanczos biconjugate A-orthonormalization method for solving dense complex non-Hermitian linear systems in realistic RCS calculation. This family of solvers shows good convergence properties, is cheap in memory as it is derived from short-term vector recurrences, is parameter-free and does not suffer from the restriction to require a symmetric preconditioner. Additionally, the CORS method does not necessitate of matrix multiplication by A^H that might be tricky to implement in some integral application codes combined with MLFMA. The results presented in this study will contribute to enhance the growing body of evidence of iterative Krylov methods for solving realistic electromagnetic scattering problems from large structures.

ACKNOWLEDGMENT

We gratefully thank the EMC Team at CERFACS in Toulouse and to EADS-CCR (European Aeronautic Defence and Space-Company Corporate Research Center) in Toulouse, for providing us with some test examples used in the numerical experiments. This research was supported by 973 Program (2007CB311002), NSFC (60973015) and the Project of National Defense Key Lab. (9140C6902030906).

REFERENCES

1. Alléon, G., S. Amram, N. Durante, P. Homsy, D. Pogarielloff, and C. Farhat, "Massively parallel processing boosts the solution of industrial electromagnetic problems: High performance out-of-core solution of complex dense systems," *Proceedings of the Eighth SIAM Conference on Parallel Computing*, M. Heath, V. Torczon, G. Astfalk, P. E. Bjrstad, A. H. Karp, C. H. Koebel, V. Kumar, R. F. Lucas, L. T. Watson, and D. E. Womble (eds.), SIAM Book, Philadelphia, Conference held in Minneapolis, Minnesota, USA, 1997.
2. Bendali, A., "Approximation par elements finis de surface de problemes de diffraction des ondes electro-magnetiques," Ph.D. thesis, Université Paris VI, 1984.
3. Bilotti, F. and C. Vegni, "MoM entire domain basis functions for

- convex polygonal patches,” *Journal of Electromagnetic Waves and Applications*, Vol. 17, No. 11, 1519–1538, 2003.
4. Carpentieri, B., I. S. Duff, and L. Giraud, “Sparse pattern selection strategies for robust Frobenius-norm minimization preconditioners in electromagnetism,” *Numerical Linear Algebra with Applications*, Vol. 7, No. 7–8, 667–685, 2000.
 5. Carpentieri, B., I. S. Duff, L. Giraud, and M. Magolu monga Made, “Sparse symmetric preconditioners for dense linear systems in electromagnetism,” *Numerical Linear Algebra with Applications*, Vol. 11, 753–771, 2004.
 6. Carpentieri, B., I. S. Duff, L. Giraud, and G. Sylvand, “Combining fast multipole techniques and an approximate inverse preconditioner for large electromagnetism calculations,” *SIAM J. Scientific Computing*, Vol. 27, No. 3, 774–792, 2005.
 7. Chew, W. C. and Y. M. Wang, “A recursive T-matrix approach for the solution of electromagnetic scattering by many spheres,” *IEEE Transactions on Antennas and Propagation*, Vol. 41, No. 12, 1633–1639, 1993.
 8. Chew, W. C. and K. F. Warnick, “On the spectrum of the electric field integral equation and the convergence of the moment method,” *Int. J. Numerical Methods in Engineering*, Vol. 51, 475–489, 2001.
 9. Danesfahani, R., S. Hatamzadeh-Varmazyar, E. Babolian, and Z. Masouri, “Applying Shannon wavelet basis functions to the Method of Moments for evaluating the Radar Cross Section of the conducting and resistive surfaces,” *Progress In Electromagnetics Research B*, Vol. 8, 257–292, 2008.
 10. Darve, E., “The fast multipole method (i): Error analysis and asymptotic complexity,” *SIAM J. Numerical Analysis*, Vol. 38, No. 1, 98–128, 2000.
 11. Dembart, B. and M. A. Epton, “A 3D fast multipole method for electromagnetics with multiple levels,” Tech. Rep. ISSTECH-97-004, The Boeing Company, Seattle, WA, 1994.
 12. Dongarra, J. J., I. S. Duff, D. C. Sorensen, and H. A. Van Der Vorst, *Numerical Linear Algebra for High-performance Computers, Software, Environments, and Tools*, Vol. 7, Society for Industrial and Applied Mathematics (SIAM), Philadelphia, PA, 1998.
 13. Durdos, R., “Krylov solvers for large symmetric dense complex linear systems in electromagnetism: Some numerical experiments,” Working Notes WN/PA/02/97, CERFACS, Toulouse, France, 2002.

14. Ergül, Ö. and L. Gürel, “Fast and accurate solutions of extremely large integral-equation problems discretized with tens of millions of unknowns,” *Electron. Lett.*, Vol. 43, No. 9, 499–500, 2007.
15. Ergül, Ö. and L. Gürel, “Efficient parallelization of the multilevel fast multipole algorithm for the solution of large-scale scattering problems,” *IEEE Transactions on Antennas and Propagation*, Vol. 56, No. 8, 2335–2345, 2008.
16. Essid, C., M. B. B. Salah, K. Kochlef, A. Samet, and A. B. Kouki, “Spatial-spectral formulation of method of moment for rigorous analysis of microstrip structures,” *Progress In Electromagnetics Research Letters*, Vol. 6, 17–26, 2009.
17. Barrett, R., et al., *Templates for the Solution of Linear Systems: Building Blocks for Iterative Methods*, SIAM, 1995.
18. Fan, Z., D.-Z. Ding, and R.-S. Chen, “The efficient analysis of electromagnetic scattering from composite structures using hybrid CFIE-IEFIE,” *Progress In Electromagnetics Research B*, Vol. 10, 131–143, 2008.
19. Freund, R. W., “A transpose-free quasi-minimal residual algorithm for non-Hermitian linear systems,” *SIAM J. Scientific Computing*, Vol. 14, No. 2, 470–482, 1993.
20. Freund, R. W. and N. M. Nachtigal, “QMR: A quasi-minimal residual method for non-Hermitian linear systems,” *Numerische Mathematik*, Vol. 60, No. 3, 315–339, 1991.
21. Freund, R. W. and N. M. Nachtigal, “An implementation of the QMR method based on coupled two-term recurrences,” *SIAM J. Scientific Computing*, Vol. 15, No. 2, 313–337, 1994.
22. Freund, R. W., “Conjugate gradient-type methods for linear systems with complex symmetric coefficient matrices,” *SIAM J. Sci. Stat. Comput.*, Vol. 13, No. 1, 425–448, 1992.
23. Gan, H. and W. C. Chew, “A discrete BiCG-FFT algorithm for solving 3-D inhomogeneous scatterer problems,” *Journal of Electromagnetic Waves and Applications*, Vol. 9, No. 10, 1339–1357, 1995.
24. Gibson, W. C., *The Method of Moments in Electromagnetics*, Chapman & Hall/CRC, Boca Raton, FL, 2008.
25. Greenbaum, A., *Iterative Methods for Solving Linear Systems*, No. 17. Frontiers in Applied Mathematics, SIAM, Philadelphia, 1997.
26. Greengard, L. and V. Rokhlin, “A fast algorithm for particle simulations,” *Journal of Computational Physics*, Vol. 73, 325–348, 1987.

27. Hassani, H. R. and M. Jahanbakht, "Method of Moment analysis of finite phased array of aperture coupled circular microstrip patch antennas," *Progress In Electromagnetics Research B*, Vol. 4, 197–210, 2008.
28. Ipsen, I. C. F. and C. D. Meyer, "The idea behind Krylov methods," Tech. Rep. CRSC-TR97-3, NCSU Center for Research in Scientific Computation, To Appear in *American Mathematical Monthly*, Jan. 31, 1997.
29. Jing, Y.-F., T.-Z. Huang, Y. Zhang, L. Li, G.-H. Cheng, Z.-G. Ren, Y. Duan, T. Sogabe, and B. Carpentieri, "Lanczos-type variants of the COCR method for complex nonsymmetric linear systems," *Journal of Computational Physics*, Vol. 228, No. 17, 6376–6394, 2009.
30. Lee, J., C.-C. Lu, and J. Zhang, "Sparse inverse preconditioning of multilevel fast multipole algorithm for hybrid integral equations in electromagnetics," Tech. Rep. 363-02, Department of Computer Science, University of Kentucky, KY, 2002.
31. Lee, J., C.-C. Lu, and J. Zhang, "Incomplete LU preconditioning for large scale dense complex linear systems from electromagnetic wave scattering problems," *J. Comp. Phys.*, Vol. 185, 158–175, 2003.
32. Lee, J., C.-C. Lu, and J. Zhang, "Sparse inverse preconditioning of multilevel fast multipole algorithm for hybrid integral equations in electromagnetics," *IEEE Transactions on Antennas and Propagation*, Vol. 52, No. 9, 2277–2287, 2004.
33. Li, J. Y., L. W. Li, and Y. B. Gan, "Method of Moments analysis of waveguide slot antennas using the EFIE," *Journal of Electromagnetic Waves and Applications*, Vo. 19, No. 13, 1729–1748, 2005.
34. Lin, J. H. and W. C. Chew, "BiCG-FFT T-matrix method for solving for the scattering solution from inhomogeneous bodies," *IEEE Trans. Microwave Theory Tech.*
35. Malas, T., Ö. Ergül, and L. Gürel, "Sequential and parallel preconditioners for large-scale integral-equation problems," *Computational Electromagnetics Workshop*, 35–43, Izmir, Turkey, Aug. 30–31, 2007.
36. Malas, T. and L. Gürel, "Incomplete LU preconditioning with multilevel fast multipole algorithm for electromagnetic scattering," *SIAM J. Scientific Computing*, Vol. 29, No. 4, 1476–1494, 2007.
37. Mittra, R. and K. Du, "Characteristic basis function method for iteration-free solution of large method of moments problems,"

- Progress In Electromagnetics Research B*, Vol. 6, 307–336, 2008.
38. Nilsson, M., “Iterative solution of Maxwell’s equations in frequency domain,” Master’s thesis, Uppsala University Department of Information Technology.
 39. Rahola, J. and S. Tissari, “Iterative solution of dense linear systems arising from the electrostatic integral equation in MEG,” *Physics in Medicine and Biology*, Vol. 47, No. 6, 961–975, 2002.
 40. Rao, S. M., D. R. Wilton, and A. W. Glisson, “Electromagnetic scattering by surfaces of arbitrary shape,” *IEEE Trans. Antennas Propagat.*, Vol. 30, 409–418, 1982.
 41. Saad, Y., “A flexible inner-outer preconditioned GMRES algorithm,” *SIAM J. Scientific and Statistical Computing*, Vol. 14, 461–469, 1993.
 42. Saad, Y., *Iterative Methods for Sparse Linear Systems*, PWS Publishing, New York, 1996.
 43. Saad, Y. and M. H. Schultz, “GMRES: A generalized minimal residual algorithm for solving nonsymmetric linear systems,” *SIAM J. Scientific and Statistical Computing*, Vol. 7, 856–869, 1986.
 44. Samant, A. R., E. Michielssen, and P. Saylor, “Approximate inverse based preconditioners for 2D dense matrix problems,” Tech. Rep. CCEM-11-96, University of Illinois, 1996.
 45. Sertel, K. and J. L. Volakis, “Incomplete LU preconditioner for FMM implementation,” *Micro. Opt. Tech. Lett.*, Vol. 26, No. 7, 265–267, 2000.
 46. Sleijpen, G. L. G. and D. R. Fokkema, “BiCGstab(ell) for linear equations involving unsymmetric matrices with complex spectrum,” *ETNA*, Vol. 1, 11–32, 1993.
 47. Sogabe, T., “Extensions of the conjugate residual method,” Ph.D. thesis, University of Tokyo, 2006.
 48. Sogabe, T., M. Sugihara, and S.-L. Zhang, “An extension of the conjugate residual method to nonsymmetric linear systems,” *J. Comput. Appl. Math.*, Vol. 226, 103–113, 2009.
 49. Song, J. M. and W. C. Chew, “The fast illinois solver code: Requirements and scaling properties,” *IEEE Computational Science and Engineering*, Vol. 5, No. 3, 19–23, 1998.
 50. Song, J. M., C.-C. Lu, and W. C. Chew, “Multilevel fast multipole algorithm for electromagnetic scattering by large complex objects,” *IEEE Transactions on Antennas and Propagation*, Vol. 45, No. 10, 1488–1493, 1997.
 51. Song, J. M., C. C. Lu, W. C. Chew, and S. W. Lee, “Fast illinois

- solver code (FISC),” *IEEE Antennas and Propagation Magazine*, Vol. 40, No. 3, 27–34, 1998.
52. Sonneveld, P., “CGS, a fast Lanczos-type solver for nonsymmetric linear systems,” *SIAM J. Scientific and Statistical Computing*, Vol. 10, 36–52, 1989.
 53. Su, D. Y., D.-M. Fu, and D. Yu, “Genetic algorithms and method of moments for the design of PIFAs,” *Progress In Electromagnetics Research Letters*, Vol. 1, 9–18, 2008.
 54. Sylvand, G., “La méthode multipôle rapide en électromagnétisme: Performances, parallélisation, applications,” Ph.D. thesis, Ecole Nationale des Ponts et Chaussées, 2002.
 55. Sylvand, G., “Complex industrial computations in electromagnetism using the fast multipole method,” *Proceedings of Waves 2003*, P. Joly, P. Neittaanmaki, G. C. Cohen, E. Heikkola (eds.), *Mathematical and Numerical Aspects of Wave Propagation*, 657–662, Springer, 2003.
 56. Van Der Vorst, H. A., “Bi-CGSTAB: A fast and smoothly converging variant of Bi-CG for the solution of nonsymmetric linear systems,” *SIAM J. Scientific and Statistical Computing*, Vol. 13, 631–644, 1992.